Amplitude-equation formalism for four-wave-mixing geometry with transmission gratings

D. Engin, M. C. Cross,* and A. Yariv

Department of Applied Physics, California Institute of Technology, 128-95, Pasadena, California 91125

An amplitude equation is derived for a four-wave-mixing geometry with nearly counterpropagating, mutually incoherent, nondiffracting pump beams, spatially overlapping in a photorefractive material with a nonlocal response. This equation extends the earlier linear two-dimensional theory to the weakly nonlinear regime. The analysis also starts from a more complete equation for the photorefractive effect, which leads to the prediction of novel effects especially apparent in the nonlinear regime. Precise predictions for the spatio-temporal behavior of the grating amplitude in the nonlinear regime are presented. The range of validity of the amplitude equation is studied. The characteristics of the instability in the nonlinear regime are analyzed through a front-selection analysis. © 1997 Optical Society of America [S0740-3224(97)01812-2]

1. INTRODUCTION

The four-wave mixing geometry considered in this paper is illustrated in Fig. 1. Two mutually incoherent, nearly counterpropagating, nondiffracting pump beams are incident to a photorefractive crystal. Since the two pump beams are mutually incoherent, they cannot write reflection gratings. However, each beam, in the absence of the other, is unstable and fans, i.e., the noise present that is due to imperfections in the material gets amplified, resulting in noisy transmission gratings and a broad angular scattering of the incident beam. When the two beams are present the instability becomes much more selective. The selectivity arises owing to an efficient grating-sharing process. In Fig. 1, for each pump beam there is a large set of possible transmission gratings that can become unstable. But only one grating (for plane-wave pumps), which corresponds to a unique wave number, belongs to both of these sets, i.e., it is shared by the counterpropagating waves. The above geometry was considered for the first time as a model for the double-phase-conjugate mirror in the one-dimensional (1D) theory.[1] The theory involved the efficient coupling of counterpropagating plane waves through the single shared grating.

Recently we have found theoretically and measured experimentally[2] that the dynamics of the instability exhibit critical slowing down at the instability threshold, and an analogy between the mean-field theory for ferromagnetism and the (1D) theory was drawn. In this paper we extend the analogy by deriving an amplitude equation[3] for the instability. This is a unified approach to systems that exhibit critical transitions, and it has successfully quantified a number of experimental observations in these physical systems.[3] The equation governs the spatial dynamics of the grating in the weakly nonlinear regime (near the threshold) and many of the important characteristics of the above instability, e.g., the convective behavior and the critical slowing down, can easily be deduced from it. Also, more exact, numerical calculations of the grating amplitude [two-dimensional (2D)] in the nonlinear regime are straightforward through the amplitude equation.

Similar four-wave-mixing geometries have been considered in other analytical[4–6] and numerical[7,8] models for the double-phase-conjugate mirror. Numerical models study primarily the more practical issues such as phase-conjugation fidelity. Most of the theoretical studies have been scalar theories; however, a vectorial approach has also been employed.[6] The scalar analytical theories[1,4,5] differ in the characteristics of the pump beams considered, i.e., nondiffracting versus speckled pump beams. Our approach here is classified as one of nondiffracting pump beams. The amplitude equation extends the earlier 2D analytical theories[4] to the nonlinear regime. Also, this approach allows the treatment of a more complete photorefractive material equation[7] than those treated in the earlier analytical studies.

The outline of the paper is as follows: We first introduce the starting equations, which consist of a comprehensive equation for the space-charge field (derived from Kukhtarev's equations) and the paraxial wave equations for the counterpropagating beams. In Section 2 the linear-stability spectrum is derived. This is an intuitive generalization of the 1D theory to the 2D theory, and it captures the convective nature of the instability.[4] The amplitude equation is introduced in Section 4. This equation is of the form of a complex Ginzburg–Landau equation. The vast literature[3] that already exists for this nonlinear equation allows us to extend the linear physical picture presented in Section 4 to the nonlinear regime. The expected spatial dynamics of the grating amplitude in the nonlinear regime is described in Section 5. Precise predictions for the spatio-temporal behavior of the grating amplitude are presented through the linear front-selection analysis. The analysis is applied both to the starting equations and to the amplitude equation, and the range of validity of the amplitude equation is discussed. In this section we also investigate the possibility of a transition from convective to absolute instability, and we

discuss the implications of this study for the nature of the instability in the nonlinear regime. In Section 6, we present a detailed summary emphasizing the main results of this study.

2. STARTING EQUATIONS

The propagation of nearly counterpropagating, monochromatic optical waves in photorefractive materials is governed by the following equations:

$$ie - i\alpha^2\partial_x^2 e + \alpha\partial_x i$$

$$= -(1 + \alpha\partial_x e)^2\partial_t e - ei\alpha\partial_x e - \alpha\partial_x i\partial_x e, \quad (1a)$$

$$\exp[j(kL - \beta)z](\partial_z A - j\beta A - j\beta\partial_x^2 A + j2\gamma_0 eA) + \text{c.c.}$$

$$= 0, \quad (1b)$$

$$\exp[-j(kL - \beta)z](\partial_z B + j\beta B + j\beta\partial_x^2 B - j2\gamma_0 eB) + \text{c.c.}$$

$$= 0. \quad (1c)$$

Here, z, x, t are normalized by the length of the interaction region L, the inverse of the transverse component of the wave number for the pump beams q_0 and the dielectric relaxation time τ_d, respectively. The space-charge field, $e = E_{sc}q/(k_B T k_D)$ is normalized by the amplitude of the maximum field possible, which occurs when the grating wave number is equal to the Debye wave number, k_D.[9] The intensity profile that is due to the counterpropagating incoherent beams, i, is normalized by the conserved total incident intensity, and the beam amplitudes are normalized by the incident pump-beam amplitude. [Note that in this article j refers to $(-1)^{1/2}$.] Only the degenerate case with equal pump intensities is considered. Another important point is that A, B are complex amplitudes while e, i are real amplitudes.

Equation (1a) can be derived from Kukhtarev's equations[7,10] for $N_A \ll N_D$ and for fast electronic recombination. Here, only the nonlocal response of the material owing to charge transport is considered. A brief description of the derivation of Eq. (1a) is presented in Appendix B. Equations (1b) and (1c) are the paraxial-wave equations for the counterpropagating beams. The magnitudes of the parameters $\alpha = q_0/k_D$ and β
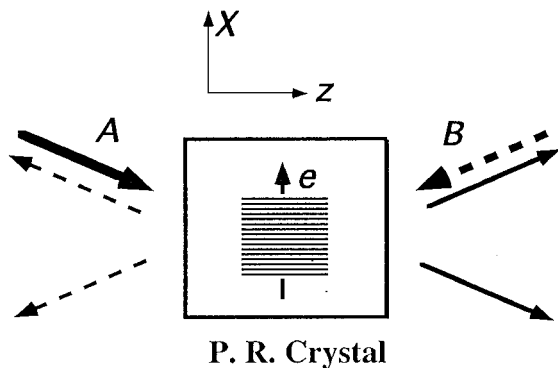

P. R. Crystal

Fig. 1. 2D four-wave-mixing geometry in a photorefractive crystal: Two nearly counterpropagating, mutually incoherent pump beams are denoted by thick-solid and thick-dashed arrows. The waves traveling to the right (solid arrows) and the waves traveling to the left (dashed arrows) interact through a set of shared transmission gratings.

$= (q_0/2k)q_0 L$ reflect the relative importance of the transverse spatial derivatives in Eqs. (1), owing to the grating-wave-number dependence of the photorefractive effect and to wave propagation, respectively. For typical experimental conditions for phase conjugation, β is orders of magnitude larger than α ($\beta \approx 2 \times 10^3$, $\alpha \leqslant 1$). When $2q_0$ is considered to be a grating wave number (see Section 3) then the β parameter can be shown to be proportional to the Q parameter[11] of the particular volume hologram. Thus a large β value signifies a thick hologram. In Eqs. (1b) and (1c), we define the control parameter $\gamma_0 = (Lk/2n_b)r(k_D k_B T/q)$,[7] where r is the effective electro-optic coefficient. In this article the slow dependence of r on the grating wave number is neglected.

3. LINEAR-STABILITY ANALYSIS

The linear-stability analysis is a straightforward generalization of the linearized 1D theory. It captures the convective nature of the instability in a simple way and renders the source of this behavior easier to trace. There have been earlier studies of the same problem,[4,12] however, those studies start with a simpler material equation and ignore the effects of the grating-wave-number dependence of the photorefractive effect. Our results agree with them in the simplified limits.

In the analysis the pump waves are taken to be nearly counterpropagating plane waves (Fig. 1), and we consider a system with infinite transverse size. The linearized 1D theory[1] takes into account only the efficiently shared, phase-matched grating, which we will refer to as the phase-conjugate mode. The theory finds that the grating becomes unstable (an exponential growth in time) above a threshold value for the coupling constant, i.e., the growth rate of the grating goes from a negative value to a positive value crossing the threshold (critical slowing down[2]). It also finds that the phase velocity of this most unstable grating is zero, and the spatial growth of the phase-conjugate waves from the longitudinal boundaries is linear instead of exponential in z. From these results the theory concludes that the system is an oscillator (also known as an absolute instability). The transverse dimension can be added to this theory by simply considering a slow transverse modulation to the most unstable grating. The analysis includes other possible gratings that have slightly larger or smaller wave numbers. These modes can become unstable through an imperfect grating-sharing mechanism: For these modes the gratings written by the counterpropagating waves have slightly different wave vectors, and hence the diffraction of the pumps from each other's gratings are phase mismatched [Fig. 2(b)]. For a system with finite interaction length the phase mismatch is allowed, and for a slightly larger coupling constant these nearby modes become unstable.

A classification of the instability based on the existence of a threshold (change of sign for the growth rate) or z dependence of the phase-conjugate-wave amplitudes can be misleading. A correct classification of the instability requires the study of the entire spectrum of unstable modes. To illustrate the differences between an absolute instability and a convective instability, it is instructive to con-

sider a noise source with a broad spatial spectrum. The source is spatially localized in the infinite transverse system, and it is turned on and off in a short time (Fig. 3). From this noise only the grating modes that are unstable will start growing in time. Thus a wave packet will develop with a spatial spectrum that corresponds to the set of unstable modes. The characteristics of the motion of this wave packet are governed by the linear-stability spectrum, which is the relevant dispersion relationship. If the wave packet is stationary in space, then the grating amplitude locally grows exponentially in time, and the system is called an oscillator (absolute instability) [Fig. 3(a)]. However, if the wave packet not only grows exponentially in time but also moves in some direction, then locally the grating amplitude decays, and the system is called an amplifier (convective instability) [Fig. 3(b)]. In terms of these definitions, a nonzero group-velocity term in the linear-stability spectrum translates into a convective system, since the finite-propagation speed always overcomes the slow exponential growth near threshold.

The above classification of the instability has important consequences when a finite transverse system is considered. In the convective case, the disturbance that grows most strongly is the amplified noise from one of the transverse boundaries, and the developed grating is sensitive to temporal fluctuations in the boundary noise. In an absolutely unstable system the transverse boundaries are not as critical in determining the characteristics of the growing grating amplitude. The linear-stability spectrum is crucial to distinguish between the oscillator and amplifier case, and we now describe its derivation.

We consider a slow transverse modulation of the most unstable grating wave number q_c, which is $q_c = 2$ in the normalized notation:
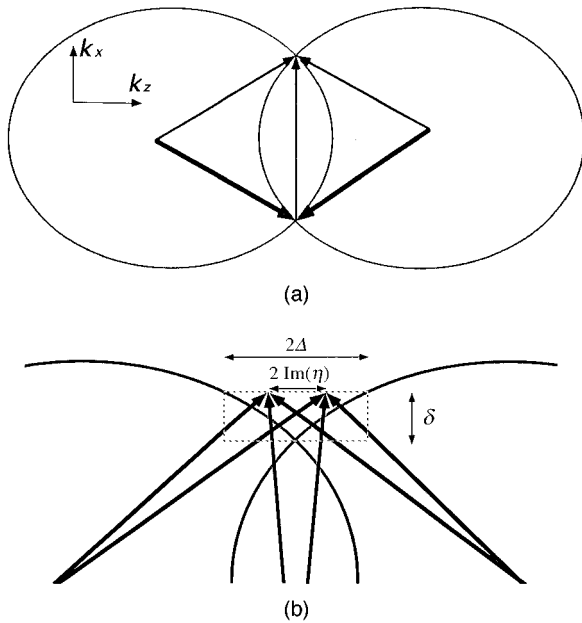

(a)

(b)

Fig. 2. k-space configuration of the interacting waves and the grating wave vector: (a), 1D theory (phase-conjugate mode) and efficient grating sharing with optimal phase matching; (b), transverse modulation δ added to the phase-conjugate mode, resulting in an inefficient grating-sharing process in which phase matching is not complete. Thick-solid arrows, pump waves; thin-solid arrows, scattered waves and the grating-wave vector.
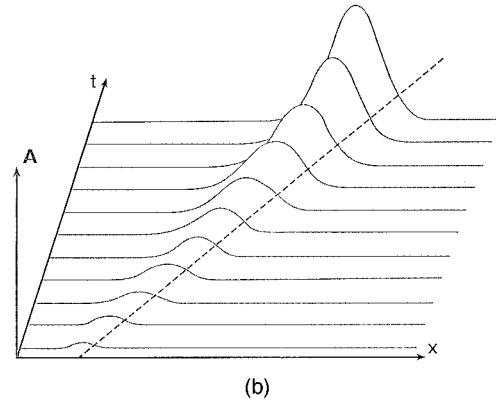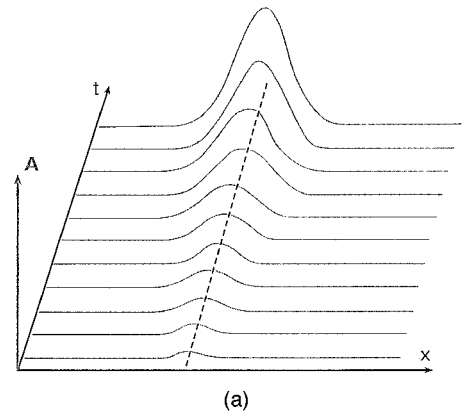

(a)

(b)

Fig. 3. Spatio-temporal behavior of the grating amplitude in the linear regime (for an infinite transverse system, with localized noise source turned on for a short time): (a), absolute instability (oscillator); (b), convective instability (amplifier). The x,t coordinates of the peak of the amplitude are shown by the dashed line.

$$e = \exp[j(2 + \delta)x]\exp(-j\Omega t)\bar{e}_\delta(z) + \text{c.c.} \quad (2a)$$

The waves consist of the undepleted pumps and the scattered plane waves from the modulated grating:

$$A = \exp(-jx) + \exp[j(1 + \delta)x]\exp(-j\Omega t)\bar{a}_\delta(z) + \text{c.c.} \quad (2b)$$

$$B = \exp(-jx) + \exp[j(1 + \delta)x]\exp(-j\Omega t)\bar{b}_\delta(z) + \text{c.c.} \quad (2c)$$

Here Ω is the complex frequency and defines the linear-stability spectrum. Looking for solutions of this form in Eqs. (1), we arrive at the following linear system:

$$\begin{bmatrix} 1 & j\tilde{\gamma}/2 & j\tilde{\gamma}/2 \\ j2\gamma_0 & \partial_z + \Delta & 0 \\ -j2\gamma_0 & 0 & \partial_z - \Delta \end{bmatrix} \begin{bmatrix} \bar{e}_\delta \\ \bar{a}_\delta \\ \bar{b}_\delta \end{bmatrix} = 0, \quad (3)$$

with the boundary conditions $\bar{a}_\delta(0) = 0$, $\bar{b}_\delta(1) = 0$. Here the dephasing factor $\Delta = j\beta(\delta^2 + 2\delta)$ is the degree of phase mismatch between the shared grating and the scattered waves. In the 1D theory the dephasing factor is zero since the shared grating is perfectly phase matched [Fig. 2(a)]. We define $\tilde{\gamma} = \alpha(2 + \delta)/\{-j\Omega + 1 + [\alpha(2 + \delta)]^2\}$, which captures the wave-number dependence of the two-wave-mixing gain, Γ.[1] In our notation Γ is given by $2\gamma_0\tilde{\gamma}$. Also note that $-j\tilde{\gamma}/2$ is the ratio between the space-charge-field amplitude and the spa-

tially varying intensity pattern. The 1D theory consistently shows that this ratio is purely imaginary ($\pi/2$ for the phase-shifted grating), and hence the phase velocity of the grating is zero.

The system of ordinary differential equations is solved by assuming an exponential solution and finding the eigenvalues (exponents of the spatial growth) and eigenvectors of the resulting linear system. In this way the pair of complex eigenvalues η, $-\eta$ are given by $\eta^2 = \Gamma\Delta + \Delta^2$, and the most general solutions are of the forms

$$\bar{a}_\delta = \Gamma/2 C_1 \exp(\eta z) + \Gamma/2 C_2 \exp(-\eta z), \tag{4a}$$

$$\bar{b}_\delta = (\eta - \Delta - \Gamma/2)C_1 \exp(\eta z) - (\eta + \Delta + \Gamma/2)C_2$$
$$\times \exp(-\eta z), \tag{4b}$$

$$\bar{e}_\delta = -j\tilde{\gamma}[(\eta - \Delta)C_1 \exp(\eta z) - (\eta + \Delta)C_2 \exp(-\eta z)]. \tag{4c}$$

The k-space picture for nonzero modulation δ is shown in Fig. 2(b). Notice that in Fig. 2(b) the scattered wave vectors are not on the index ellipsoid; this points out the nonzero phase velocity for the particular mode. The scattered waves have optical frequencies that are slightly different from those of the pump waves. The boundary conditions fix the phase between the two evanescent waves at positions $z = 0$ and $z = 1$, and this allows only a certain band of eigenvalues. In other words, Γ must be a function of Δ through the following transcendental equation:

$$-2/\Gamma = \sinh(\eta)/\eta \tag{5}$$

Equation (1a) can be written in the following manner:

$$-j\Omega = -1 - \alpha^2(2 + \delta)^2 - \gamma_0\alpha(2 + \delta)(-2/\Gamma), \tag{6}$$

and with $\Gamma(\Delta)$ from Eq. (5), this gives a convenient expression for the linear-stability spectrum. Notice that the modulation δ dependence coming from the wave propagation through $\Gamma(\Delta)$ and from the photorefractive effect (the terms involving α) are separable.

Close to the threshold we expect only the modes very near to the phase-conjugate mode to become unstable. It is then instructive to derive an expansion of the spectrum for slow modulation of the phase-conjugate mode. The expansion of $1/\Gamma$ for small Δ can be evaluated by assuming an expansion in Eq. (5) and solving the resulting set of equations for the coefficients iteratively, to yield

$$-2/\Gamma = 1 + \Delta/3 + 4/45\,\Delta^2 + 19/945\,\Delta^3 + 8/2025\,\Delta^4$$
$$+ O(\Delta^5). \tag{7}$$

Using this expansion, the stability-spectrum Eq. (6) takes the following form:

$$\mathrm{Re}(-j\Omega) = -(1 + \alpha^24 + 2\alpha\gamma_0) - \delta(\alpha^24 + \alpha\gamma_0)$$
$$+ \delta^2(32/45\,\alpha\gamma_0\beta^2 - \alpha^2) + O(\delta^3), \tag{8a}$$

$$\mathrm{Im}(-j\Omega) = -\delta(4/3\,\alpha\gamma_0\beta) - \delta^2(4/3\,\alpha\gamma_0\beta) + O(\delta^3). \tag{8b}$$

The real part of the stability spectrum corresponds to the exponential growth or decay rate of the amplitude of the unstable mode, while the part of the imaginary term proportional to δ is the group-velocity term. The nonzero

group velocity in the x direction classifies the instability as a convective one. For typical experimental parameters for phase conjugation, the angle between the two pump beams is a few degrees. For this regime typically β is a few orders of magnitudes larger than α and the real part of the linear-stability spectrum can be conveniently expressed as

$$\mathrm{Re}(-j\Omega) = -2\alpha(\gamma_0 - \gamma_{0c})$$
$$+ 32/45\,\beta^2\delta^2\alpha\gamma_0 + O(\beta^3\delta^3), \tag{9}$$

where $\gamma_{0c} = -(1 + 4\alpha^2)/(2\alpha)$ is the threshold value for the control parameter, corresponding to the two-wave-mixing gain of -2. Notice that for zero spatial modulation the real part of the spectrum changes sign as the control parameter is increased (becomes more negative) above the threshold value (as predicted by the 1D theory). Figure 4 illustrates the band of modes located around the phase-conjugate mode, which becomes unstable as the threshold is crossed. The band has a maximum at the phase-conjugate mode, and the quadratic drop in the growth rate away from this mode is dominated by the phase-mismatching effect.

Although the phase-conjugate mode has zero phase velocity [Eq. (8)], the group velocity is nonzero. Thus, as illustrated in Fig. 3(b), a grating wave packet consisting of these unstable spatial modes in an infinite transverse system would propagate toward the positive-x direction. For a dielectric relaxation time of 1 s and a grating period of 2 μm, the group velocity is about 0.1 cm/s. For the four-wave-mixing system the noise is thought to be due to the scattering of the pump beams from stationary imperfections in the material, and hence it is independent of time.[13] In this case it is instructive to consider a semi-infinite system with spatially distributed, time-independent noise [Fig. 7(b), small t]. In this system, the noise at the lower boundary ($x = 0$) is amplified the most as the disturbance propagates to positive x, effectively outlining an exponentially growing envelope. So although the z dependence of the phase-conjugate waves is linear, an exponential x dependence is expected in the linear regime. A finite transverse interaction region, which usually comes about owing to the finite size of the pump beams, can be conveniently modeled in this simple picture with an absorbing transverse boundary to the positive-x side of the first boundary. The noise-generated disturbance grows and propagates through the interaction region, only to be eventually absorbed by the right boundary. For a typical group velocity of 0.1 cm/s and transverse width (width of the pump beams) of 1 mm, the disturbance crosses the interaction region in 1 s. The exponential envelope is one of the first sought-after predictions of the convective behavior (in the context of large scale distortions in the phase-conjugate beams).[14] We note that the absorbing nature of the second boundary is assumed here for simplicity. However this assumption does not change the main conclusions of this article.

For the large β regime, the wave-number dependence of the photorefractive effect is important only for determining the threshold value of γ_0 [Eq. (9)], however, notice that effectively the two-wave-mixing gain threshold, $\Gamma = -2$, remains the same. A very important point in Eq.

(9) is that the spectrum can be expressed as a function of $\delta\beta$ in this regime, and the above expansion is good only for small $\delta\beta$. This point will become important for understanding the range of validity of the amplitude equation. Also notice that in Fig. 4 the growth rate is plotted as a function of $\delta\beta$; in this way the dependence of the results on β (angle between the pump beams) can be scaled out.

As the angle between the two pump beams becomes smaller, the magnitude of β becomes closer to unity, and the effects of the grating-wave-number dependence of the coupling constant becomes more important. Figure 5 illustrates the effects on the real part of the spectrum for different α values. The most unstable mode now deviates from the phase-conjugate mode. It is found that the most unstable mode is pulled toward the maximum of $\tilde{\gamma}$, which corresponds to the grating wave number equaling the Debye wave number. This shift also yields a less negative threshold than expected with γ_{0c}. A more dramatic deviation from the phase-conjugate mode was observed with materials with mixed (local and nonlocal) responses.[15] The leading-order corrections to the threshold value and the most unstable mode can be calculated through a straightforward perturbation analysis. The results are the following:

$$\gamma_{1c} = \gamma_{0c} + (1 - 4\alpha^2)^2/(1 + 4\alpha^2)45/128\ 1/\beta^2$$
$$+ O(1/\beta^4), \tag{10a}$$

$$\delta_{1c} = (1 - 4\alpha^2)/(1 + 4\alpha^2)45/64\ 1/\beta^2 + O(1/\beta^4), \tag{10b}$$

$$\nu_{1c} = (1 - 4\alpha^2)/(1 + 4\alpha^2)15/16\ \alpha/\beta + O(1/\beta^3). \tag{10c}$$

Since the most unstable mode is not the phase-conjugate mode in this regime a finite phase velocity for this grating can be calculated from Eqs. (8b) and (10b).

For dielectric relaxation times of a duration of microseconds the phase velocity should be measurable through
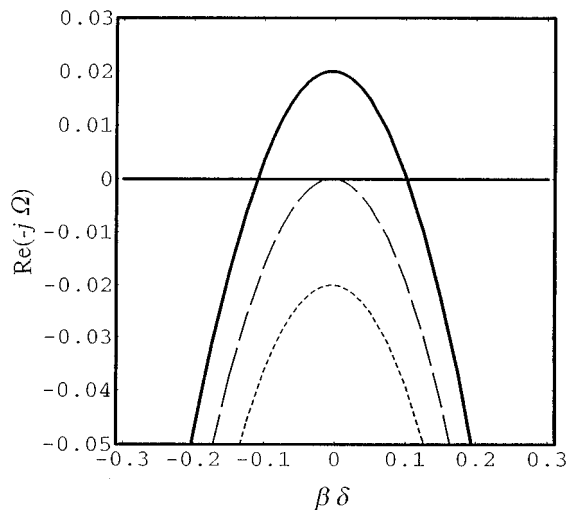

Fig. 4. Growth rate (the real part of the linear-stability spectrum) versus modulation wave number around the phase-conjugate mode for $\beta = 100$, $\alpha = 1$: below the threshold, $\gamma_0 = 2.49$ (short-dashed curve); at the threshold, $\gamma_0 = 2.50$ (long-dashed curve); above the threshold, $\gamma_0 = 2.51$ (solid curve).
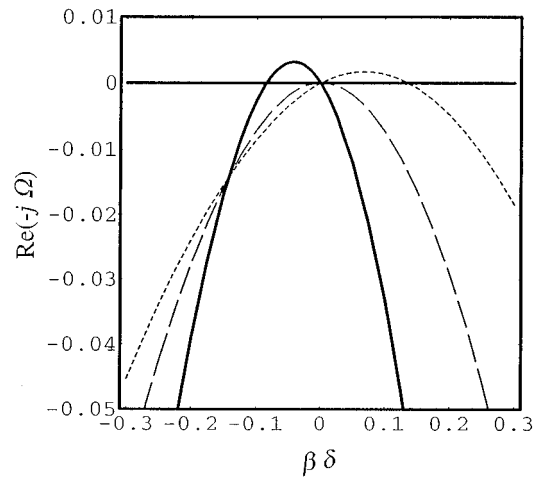

Fig. 5. Effects of the wave-number dependence of the photorefractive effect on the growth rate. Growth rate (the real part of the linear-stability spectrum) versus modulation wave number around the phase-conjugate mode for $\gamma_0 = \gamma_{0c}(\alpha)$: $\beta = 10$, $\alpha = 1/20$ (short-dashed curve); $\beta = 10$, $\alpha = 1/2$ (long-dashed curve); $\beta = 10$, $\alpha = 1$ (solid curve).

an interference experiment between the phase-conjugate and the pump beams. It is important to note that for a complete quantitative study of the regime with very small angles between the two pump beams (with the pump beams almost counterpropagating) two additional scattered plane-wave amplitudes need to be considered.[16] It can be shown, in approaching this regime, that the correction terms to the stability spectrum are proportional to Γ/β^2, and hence as β approaches unity the complete problem needs to be solved. However, we expect the basic qualitative picture of increasing deviation from the phase-conjugate mode to remain.

4. AMPLITUDE EQUATION

In Section 3 the linear-stability spectrum that governs the linear spatio-temporal behavior of the system is derived, and its implications are described. In this section we will introduce the amplitude equation, which extends the linear theory to the weakly nonlinear regime. Here we attempt to motivate the form of the amplitude equation through physical arguments. A rigorous derivation of this equation from the starting equations, Eqs. (1), can be found in Appendix A.

As shown in Fig. 4, near the instability threshold we find that only a small family of the modes around the phase-conjugate mode becomes unstable and contributes to a growing instability, as depicted in Fig. 3(b). Hence, near the threshold, the first few terms of the small modulation $\delta\beta$ expansion of the dispersion relationship, Eqs. (8), are expected to govern the spatio-temporal behavior of the growing instability. At the same time in this regime, weak nonlinearities are expected to result in the saturation of the exponentially growing disturbance. The balance between these effects are described by the amplitude equation

$$\tau_0\partial_t A + \tau_0 s_0\partial_x A = \varepsilon A + 2s + \xi_0^2(1 + jc_1)\partial_x^2 A$$
$$- g_0|A|^2 A. \tag{11}$$

The derivation (see Appendix A) utilizes a multiple-scale perturbative approach. In the analysis, the slow temporal and spatial variables are separated by an appropriate scaling by the smallness parameter, $\varepsilon = (\gamma_0 - \gamma_{0c})/\gamma_{0c}$. Physically the slow temporal and spatial variables can be directly inferred from Fig. 4. As the threshold is crossed, the growth rate of the unstable modes changes sign, and it increases linearly with ε. This critical slowing down effect is described by the slow temporal variable. At the same time the quadratic spectrum of unstable modes, starting from a null width, widens as $\varepsilon^{1/2}$. The slow spatial variable governs the behavior of the instability amplitude that consists of this small family of unstable modes. The dependences of the wave and grating amplitudes in Eqs. (1) on the amplitude $A(x, t)$ are given by the following relations:

$$\left(\frac{\overline{A_p}}{\overline{B_p}}\right) = 1 - |A(x, t)|^2(1 + 4\alpha^2)^2/\alpha^2\left(\frac{z^2}{(1-z)^2}\right)$$
$$+ o(\varepsilon^{3/2}), \tag{12a}$$

$$\left(\begin{matrix} a \\ b \end{matrix}\right) = jA(x, t)(1 + 4\alpha^2)/\alpha\left(\frac{z}{(1-z)}\right)\exp(jx) + o(\varepsilon^{3/2}), \tag{12b}$$

$$e = A(x, t)\exp(j2x) - jA(x, t)^2 \frac{(1 + 8\alpha^2)}{2\alpha(1 + 16\alpha^2)}$$
$$\times \exp(j4x) + o(\varepsilon^{3/2}), \tag{12c}$$

where the counterpropagating waves in Eqs. (1b) and (1c) are divided into the pump and the scattered waves as

$$A = \overline{A_p}(z, t)\exp(-jx) + a(z, x, t), \tag{13a}$$

$$B = \overline{B_p}(z, t)\exp(-jx) - b(z, x, t). \tag{13b}$$

The seeding, s, [see Eq. (11)] is introduced into the problem as boundary conditions on the scattered waves at their respective input planes. In Eq. (12a), the depletion of the pump waves is apparent. The depletion is proportional to the square of the amplitude $A(x, t)$, and it increases quadratically with z starting from the waves' respective input planes. On the other hand the scattered waves are linearly proportional to the amplitude $A(x, t)$, and the waves increase in amplitude linearly with z as they traverse the interaction region. At this order we find two grating amplitudes: one with the most unstable grating wave number and another with a spatial frequency double that of the former. As described in Appendix A, the second-harmonic term arises from the nonlinearities in the material equation (1a). The second-harmonic grating should be observable with an independent phase-matched reading beam. Another interesting point is that the grating amplitude, Eq. (12c), is independent of z.

Next, we express the coefficients of the amplitude equation in terms of the system parameters. As expected the coefficients of the linear terms can be calculated from the linear-stability spectrum.

$$\tau_0^{-1} = \gamma_{0c}[\partial\gamma_0(-j\Omega)]_{0,\gamma_{0c}} = (1 + 4\alpha^2), \tag{14a}$$

$$s_0 = [\partial_\delta \operatorname{Im}(-j\Omega)]_{0,\gamma_{0c}} = (2/3)\beta(1 + 4\alpha^2), \tag{14b}$$

$$\tau_0^{-1}\xi_0^2(1 + jc_1)$$
$$= -1/2[\partial_\delta^2(-j\Omega)]_{0,\gamma_{0c}}$$
$$= \alpha^2 + 16/45\,\beta^2(1 + 4\alpha^2) + (1/3)j\beta(1 + 4\alpha^2). \tag{14c}$$

Note that the linear constants are the first few terms in the small modulation expansion of Eq. (6). They include the quadratic drop in the growth rate away from the phase-conjugate mode and the group-velocity term.

The nonlinear coefficient is given by

$$g_0 = 1/3 - (1 + 28\alpha^2 + 208\alpha^4 + 512\alpha^6)/$$
$$[1 + 16\alpha^2)4(1 + 4\alpha^2)^3].$$

The factor of one third in this expression agrees with the results of the 1D theory where the nonlinear saturation comes about owing to the depletion of the pumps. The second term in this expression is due to the nonlinear terms in the material equation (1a). Figure 6 illustrates the strong dependence of the nonlinear coefficient on α. In an experiment this dependence can be observed by measuring the slope of the reflectivity (intensity) versus two-wave-mixing gain curves for different angles between the pump beams, just above the threshold. According to the amplitude equation the slope should be inversely proportional to g_0.

An interesting advantage of the amplitude equation is the simplicity with which the finite transverse size of the interaction region can be treated (Ref. 3, Subsection 5.A). For square pump waves the finite transverse size can be modeled by simple boundary conditions for the amplitude equation. Gaussian pump beams, on the other hand, can be modeled by an amplitude equation whose linear coefficients are spatially varying. Both of these techniques assume that the introduction of the finite transverse size does not change the coefficients of the amplitude equa-
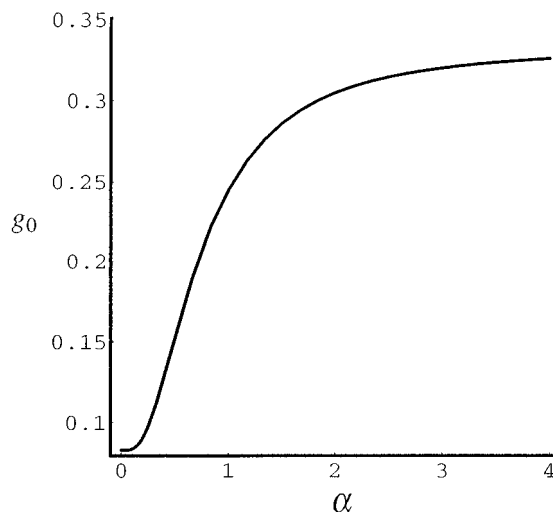

Fig. 6. Strong dependence of the nonlinear coefficient on the grating wave number; the curve shows the nonlinear coefficient, g_0, of the amplitude equation versus the ratio of the grating wave number (angle between the pump beams) and the Debye wave number, α.

tion, which were calculated for an infinite transverse system. Here we will give the necessary conditions for the correctness of this assumption. The condition is related to the small modulation expansion of the linear-stability spectrum. Clearly the first few terms of this expansion, which are included in the amplitude equation, are not sufficient if the transverse size is too small. This consideration results in the following condition: $L_x > L_z q_0/(2k)$. This condition also implies that the phase mismatch allowed, owing to the finite transverse size, is much smaller than the one allowed by the finite size in the z direction (note that this is also the case for infinite transverse size). As described in Section 3, the degree of phase mismatch allowed in the system determines the relative gain seen by the phase-conjugate mode and the nearby modes (imperfect grating sharing), and if the above condition is not met, the transverse phase mismatch is expected to contribute to the linear problem. In this article the most simple finite interaction region that can be modeled as boundary conditions for the amplitude equation is considered. Again for simplicity the two transverse boundaries are taken to be absorbing boundaries.

Last, we would like to mention some of the obvious implications of the amplitude equation. Ignoring the spatial derivatives in Eq. (11), the prediction of critical slowing down can be easily inferred analytically. The seed term in this equation goes along with the analogy drawn in Ref. 2 between 1D theory and the mean-field theory for ferromagnetism. The convective behavior is clearly reflected through the group-velocity term.

5. WEAKLY NONLINEAR REGIME

The amplitude equation introduced in Section 4 is of the form of a complex Ginzburg–Landau equation. The equation arises in many different dynamical systems, and a large amount of work has been devoted to understanding its behavior. Utilizing this body of knowledge we will generalize the qualitative dynamical picture in Fig. 3 to the weakly nonlinear regime.

We first consider a system infinite in the transverse direction, with a spatially localized noise turned on for a short time. In this case a wave packet consisting of the unstable modes grows exponentially in time and at the same time propagates in the positive-x direction with the group velocity Eq. (14b), as discussed before. Figure 7(a) illustrates the extension of the dynamics of the disturbance into the nonlinear regime. The exponential growth saturates owing to the nonlinearity, and the tails of the pulse steepen and eventually transform into fronts.[3,17] The fronts connect the uniform nonlinear state, which is a simple nonlinear plane-wave mode, to the zero-amplitude solution. The velocities of the two fronts are different from the group velocity [dashed lines in Fig. 7(a)]. The left front moves at a velocity slower than the group velocity, while the right front has a larger velocity. Effectively the width of the disturbance grows in time at a velocity equal to difference of the two front velocities. This widening of the disturbance can be thought of as the continuation of the growth process in the nonlinear regime. For larger ε (normalized coupling constant), the

difference between the velocities is expected to increase. However, in the convective regime, both fronts move in the positive-x direction, and eventually at any fixed x the disturbance is bound to decay away. Another interesting point concerns the uniform nonlinear state. The states laid down by the two fronts can be different, so that a
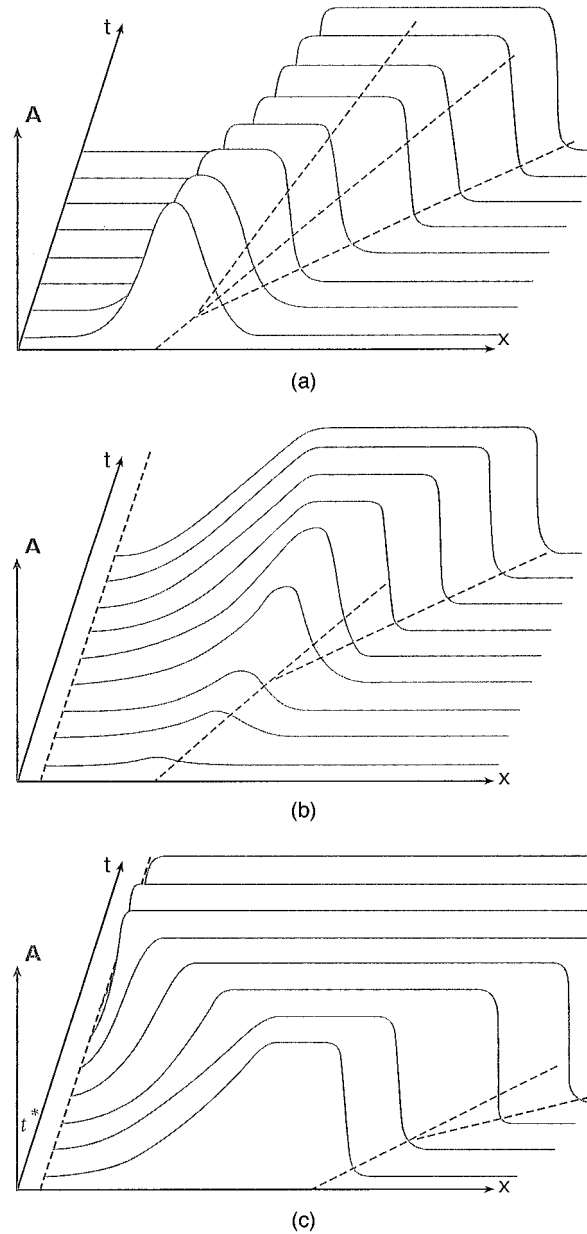

Fig. 7. Convective spatio-temporal behavior of the grating amplitude in the nonlinear regime: (a), Infinite transverse system with localized noise source, turned on for a short time; the x,t coordinates of the two fronts are shown by the dashed lines. The two fronts are traveling in the positive-x direction with velocities different from the group velocity. (b), Semi-finite transverse system with nonlocalized, time-independent noise source. Only the right front develops; the grating amplitude is the amplified noise from the left boundary. (c), Transition from convective to absolute instability in the semi-infinite system depicted in (b). At time t^* the coupling constant is increased above the transition value. A left front develops, creating a much sharper left edge for the disturbance. The grating amplitude becomes independent of the noise.

transition region between the different uniform nonlinear states may also be expected at some interior point.

In a semi-infinite system with a spatially distributed, time-independent noise source, only the right front develops [Fig. 7(b)]. At the left end of the disturbance the exponential growth from the lower boundary saturates. However, a simple front cannot form. This follows from the fact that the continuous noise source drowns out the zero-amplitude solution, which is necessary for the formation of the left front solution (moving in the negative-x direction). The length over which the solution grows to saturation at the left end, $\ln(s^{-1})\varepsilon^{-1}s_0\tau_0$, can be quite large near threshold and for small noise strength s. It should result in large scale distortions in the phase-conjugate beams, and the detailed shape can be easily calculated by a numerical solution of the amplitude equation. For typical parameters ($\tau_d = 1$ s, $\beta = 2 \times 10^4$, $s = 10^{-4}$, $2\gamma_0\widetilde{\gamma} = -3$), the length scale of the distortion is a few millimeters. Considering an upper absorbing boundary (finite-interaction region) somewhat simplifies the behavior. Eventually the moving right-front solution is absorbed by the boundary, so that the uniform nonlinear state laid down by the front solution should relax to the most unstable mode produced by the growth from the noise. In this more physical geometry with the two boundaries, the effects of the propagating front can show up only in the transients of the system. Clearly with the absorbing boundary, if the noise is turned off, the instability is eventually absorbed by the upper boundary, and the disturbance cannot be sustained.

A dramatic change can happen for a large-enough control parameter if the left-front velocity in Fig. 7(a) changes direction. Such a transition[18] might be expected since the difference between the two front solutions normally increases with increasing ε (increasing growth). Figure 7(c) illustrates the expected dynamics in the semi-infinite system, in which at time t^* the control parameter is increased above the transition value. After the control parameter is increased, a left front traveling to the negative-x direction develops. In this regime the growth dominates the advection, and the relatively steep backward-traveling front fills the region left behind by exponential growth from the left boundary. Now the healing length at the left boundary depends only on the parameters of the amplitude equation [the characteristic length $\approx \xi_0$, Eq. (14c)] and not on the size of the noise. Furthermore, in this regime, the system is absolutely unstable (an oscillator), and the grating amplitude is sustained even in the absence of noise.

The above description of the dynamical picture heavily relies on the nonlinear front solutions with characteristic velocities and spatial decay rates. Since the amplitude equation is a nonlinear partial-differential equation, multiple front solutions are expected to exist. The question of front selection in the complex Ginzburg–Landau equation[17,19] has been addressed as a generalization of the rigorous analysis by Aronson and Weinberger for the nonlinear diffusion equation.[20] It is worth pointing out that the generalization, to date, is purely heuristic. There is no completely convincing derivation of the selection results to be presented below. Nevertheless, there

are rather complete and precise predictions, and these can be tested by numerical calculations and by experiments.

A linear front-selection analysis is the simplest approach to the front-selection problem.[20] Although entailing a purely linear argument, it makes predictions for the nonlinear front solution selected at long times. A slightly more careful version is the pinch-point analysis.[21]

The analysis formulates the dynamics far in the tail of the front, where it can be expressed in terms of a superposition integral. At long times the integral is dominated by the stationary phase point, and it is required that in the frame of the selected front disturbance the amplitude neither grows nor decays in time. This leads to three different statements for the complex linear-stability spectrum,[19] $\Omega = \Omega_r + j\Omega_i$, which is now a function of the complex wave number, $\delta = q - j\kappa$. For given κ the real part of the wave number $q(\kappa)$ is chosen to maximize the growth rate,

$$\left(\frac{\partial\Omega_i}{\partial q}\right)_\kappa = 0, \tag{15}$$

yielding a one-parameter family of front velocities characterized by their asymptotic spatial decay rate, $v(\kappa) = -\Omega_i(\kappa)/\kappa$. Finally, the selected velocity is chosen to minimize $v(\kappa)$.

The amplitude equation (11) has a negative nonlinear coefficient, which classifies the bifurcation at zero ε as a supercritical one. For this case the front selected by the linear front-selection analysis is the surviving front at long times. Applying this analysis to the linear part of the amplitude equation is straightforward, and the selected wave number and velocity are as follows:

$$\kappa = -/+\varepsilon^{1/2}/[\xi_0(c_1^2 + 1)^{1/2}], \tag{16a}$$

$$q = -c_1\kappa, \tag{16b}$$

$$v = s_0+/-\varepsilon^{1/2}2\xi_0(c_1^2 + 1)^{1/2}/\tau_0. \tag{16c}$$

Here, negative κ corresponds to the right front, in Fig. 7(a). Equations (16a) and (16b) indicate that, as the control parameter is increased, the front solutions become spatially steeper, and the velocities deviate from the group velocity. Note that the difference between the velocities increase with increasing ε. For large-enough ε, the left front becomes stationary. This value of ε_a at which the transition to absolute instability occurs is given by

$$\varepsilon_a^{1/2} = s_0\tau_0/[2\xi_0(c_1^2 + 1)^{1/2}].$$

The transition value of ε_a is about 0.3, and for large β it is independent of any geometrical factors such as the angle between the pumps. The small value of ε_a is encouraging since the amplitude equation is expected to be correct near the threshold. However, calculating κ_a from Eq. (16a), one finds that $\kappa_a\beta$ is close to unity, and hence the small modulation expansion (9) may not expected to approximate Ω well.

Next we apply the linear front-selection analysis to the starting equations, Eqs. (1), and compare the results to the ones calculated from the amplitude equation. For this we have to solve Eq. (5) numerically and calculate

$(-2/\Gamma)$ as a function of the complex modulation wave number. The resulting values can be used in Eq. (6) to evaluate Ω. For large β the analysis simplifies considerably. In this regime Ω can be treated as a function of $\kappa\beta$. We are interested in κ values of order $1/\beta$. For such small values of κ, the shift in the real part of the wave number Eq. (16b) is of order $1/\beta^2$ and can be neglected. So, for a given κ, the $q(\kappa)$ that maximizes the growth rate is zero. In this case $(-2/\Gamma)$, η^2, $\Delta \approx 2\kappa\beta$ in Eq. (5) are all real and $(-2/\Gamma)$, Δ are parametric functions of η^2. For a given real value of η^2, Eq. (5) gives $(-2/\Gamma)$, which in turn can be used in $\eta^2 = \Gamma\Delta + \Delta^2$ to be solved for $2\kappa\beta$.

Figure 8 shows the family of front solutions selected for given spatial decay rate, $v(\beta\kappa)/\beta = -\Omega_i(\beta\kappa)/(\beta\kappa)$, as a function of $\kappa\beta$ for $\varepsilon = 0.05$, $\beta \approx 10^3$, $\alpha \approx 1$. Here again positive $\kappa\beta$ corresponds to the fronts moving in the negative-x direction. In this expression the geometric factor β is scaled out, and hence the results presented in Fig. 8 are independent of the angle between the pump beams. Clearly, the amplitude equation (dashed curve) works well for small $\beta\kappa$. However, for $\beta\kappa$ values close to unity and larger, the amplitude equation predicts a slower velocity for the right-front solutions and a faster velocity for the left-front solutions. Also note that an additional branch for the left fronts is attained from the starting equations. We expect that this branch may become important for the question of front selection, as will be discussed in the next section. In addition other branches with η^2 less than $-\pi^2$ can be found for the starting equations. However, as seen from Eqs. (4), these branches correspond to an oscillatory z dependence. From the viewpoint of matching the linear solution to the nonlinear uniform solution, the existence of such a front solution is unlikely, hence we neglect these branches.

According to the linear front-selection criteria the maxima of the curves in Fig. 8 correspond to the selected fronts at long times. Figure 9 illustrates the selected front velocities and spatial decay rates for different control parameter values. As shown in the lower graph of Fig. 9 the selected front velocities are at most an order of magnitude larger than the group velocity. For typical parameters ($\tau_d = 1$s, $\beta = 2 \times 10^4$), front velocities in the figure are less than 20 cm/s. For ε values less than 0.1 the predictions of the amplitude equation agree well with results obtained from the starting equations. The amplitude equation predicts a slower-moving right front for larger values of ε. For the left front, the dependence of the front velocity on ε is much weaker than expected from the amplitude equation. However the velocity difference between the two fronts continues to increase with increasing ε. As seen in the figure, the solid curve does not cross zero velocity near the parameters predicted by the amplitude equation, and hence the transition to absolute instability does not take place.

In the remaining part of this section, we compare our approach for the classification of the instability to the one used by Zozulya[4] and by Eliseev *et al.*[4] Utilizing observations from both works (both essentially employing a linear analysis) we will argue that in the large β limit and with nondiffracting pump beams the linear analysis concludes that the transition to absolute instability does not take place. Then we describe some possible nonlinear
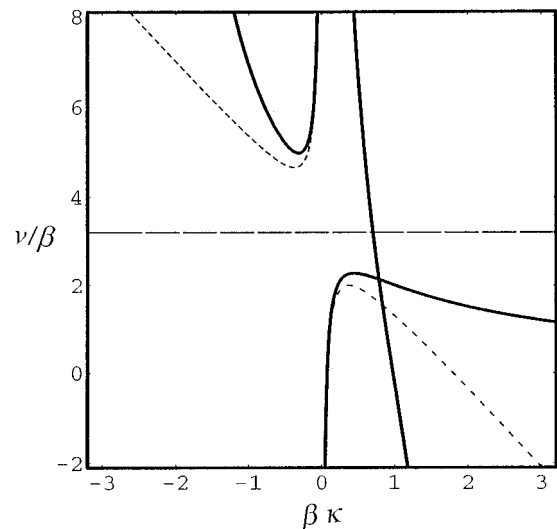

Fig. 8. Family of front solutions predicted by the marginal stability approach to the front selection for $\varepsilon = 0.05$ from the amplitude equation, Eq. (11) (short-dashed curves), and from the starting equations Eq. (1) (solid curves). The horizontal long-dashed line illustrates the group velocity. The maxima of the curves correspond to the selected front solutions for the left fronts, $\beta\kappa > 0$, and the right fronts, $\beta\kappa < 0$. There are two branches of solutions predicted by the starting equations for the left fronts.
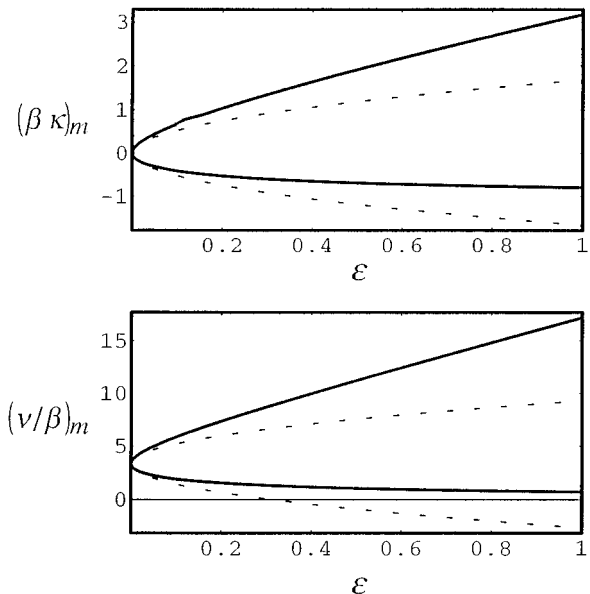

Fig. 9. Results of the linear front-selection analysis: spatial-decay rate and velocities of the selected front solutions versus normalized coupling constant ε, calculated from starting equations (solid curves) and from the amplitude equation (dashed curves).

front-selection scenarios, which the linear analysis cannot account for and which may lead to absolute instability for this simple geometry.

The two works of Ref. 4 solve the linear problem exactly for nondiffracting pump and scattered beams in two dimensions. Similar to the pinch-point analysis of the front-selection problem, the poles of the Laplace transform of the exact solution are sought. The poles dominate the long-time asymptotic of the inverse Laplace in-

tegral, and hence a pole with a positive growth rate corresponds to an absolute instability. We have approached the problem from the point of view of front selection. Applying the linear front-selection analysis, we look for saddle points of the complex linear-stability spectrum and identify the transition point as the point at which the growth rate (for the left front) at this saddle point becomes positive. It can be shown that the two analyses above lead to the same conditions on the linear-stability spectrum Eq. (15). One of the main differences in this article is the starting equations. In our analysis we treat a more complicated material equation, and we also allow the diffraction of the scattered beams, although the pump beams are nondiffracting waves. We already have shown that for the large β limit the wave-number dependence of the photorefractive effects does not greatly influence the linear problem. The diffraction term in our formulation comes about as the δ^2 term in $\Delta = j\beta(\delta^2 + 2\delta)$ [Eq. (3)]. The point is that essentially the wave-number dependence of the linear stability comes about through Δ [Eq. (6)]. The saddle points are identified as

$$\frac{d\Omega}{d\delta} = \frac{d\Omega}{d\Delta}\frac{d\Delta}{d\delta} = 0 \,. \qquad (18)$$

Hence a saddle point in δ also corresponds to a saddle point in Δ. Reference 4 proves that, for the small modulation δ limit, a saddle point in δ does not exist, and then this clearly implies the nonexistence of a saddle point in Δ. So from these observations we can conclude that even for very large modulations δ the sought-after saddle point does not exist. From the point of view of a linear analysis we conclude that a transition to absolute instability does not take place for nondiffracting pump beams.

However, front propagation is a nonlinear problem and there are examples known (see Ref. 3, Subsection 6.B.4 and Ref. 17, Subsection 4.2) where nonlinear effects lead to a different selected-front velocity than that predicted by the linear analysis. Well into the nonlinear regime there is the possibility of the selection of a different front than the one predicted by the linear analysis, and then the transition to absolute instability may take place if a left front traveling towards negative-x direction is selected, as in Fig. 7(c). The question of nonlinear front selection and front selection in situations with multi-branched dispersion curves, such as in Fig. 8, is poorly understood, and we can only point out possible scenarios for the breakdown of the linear-selection predictions. For example, in Fig. 8, we pointed out that for the starting equations (solid curves) two branches of front families are found at positive $\beta\kappa$. For an ε value of about 0.1 the value of $(\beta\kappa)_m$ for the maximum of the branch becomes larger than the $(\beta\kappa)_c$ value for the crossing point of the two branches. For larger ε values one can argue that two spatial decay rates are possible for a given front velocity. Out of the two, the smaller one will usually give the asymptotic dependence at large x. The most localized front, i.e., the one with the largest $\beta\kappa$ value, is then the one at the crossing point of the two branches and might dominate the dynamics for $\varepsilon > 0.1$ (see Ref. 19, Section 3). For $\varepsilon = 0.3$ the front velocity corresponding to the crossing point of the two branches [at $(\beta\kappa)_c$] becomes negative, and this indicates a transition to absolute insta-

bility. For typical parameters ($\tau_d = 1$ s, $\beta = 2 \times 10^4$, $s = 10^{-4}$, $\varepsilon = 0.3$) the transition should result in a behavior as depicted in Fig. 7(c), where the expected change in the rate of spatial growth from the left boundary is from 2 cm^{-1} (convective instability) to 10 cm^{-1} (absolute instability). A possible way to study the effects of such multiple front branches would be to design a simpler equation, similar to the amplitude equation, that reproduces the linear-stability-spectrum characteristics. The only certain way, however, to characterize the instability predicted by the starting equations seems to be to rely on careful numerical studies.

6. SUMMARY AND CONCLUSIONS

We have demonstrated an intuitive generalization of the 1D theory[1] to a 2D theory[4] by considering all the unstable grating modes nearby the phase-conjugate mode. The generalization leads to a dispersion relationship, the linear-stability spectrum, which captures the convective nature of the instability. We find that, for typical experimental conditions (large β), the wave-number dependence of the photorefractive effect has a small influence on the linear problem. However, as β approaches unity (very small angle between the pump beams), the effects of the photorefractive effect are expected to become much more important.

We then derive the amplitude equation for the large β limit, which extends the linear analysis into the weakly nonlinear regime. In calculating the nonlinear coefficient the higher diffraction orders can be neglected owing to the large selectivity of the most unstable volume hologram. However, the contribution from the grating components with double the spatial frequency [and from other nonlinear terms in Eq. (1a)] leads to a strong wave-number dependence for the nonlinear coefficient [Eq. (14c)]. At large angles between the pump beams the value of the coefficient approaches the one predicted by the 1D theory, where the saturation comes about owing to the depletion of the pump beams. The sign of this coefficient characterizes the bifurcation at the threshold as a supercritical one, and the nonzero group velocity immediately implies that the instability is convective (i.e., the system is an amplifier at the threshold). The amplitude equation then provides an easy formulation for calculating the spatial distribution of the noise-driven solution in this regime, including the nonlinear saturation.

The possibility of a transition to an absolute instability is discussed in terms of selection criteria for the propagation velocity of a nonlinear front (the building block for constructing a physical picture for the spatial dynamics in the nonlinear regime). The simplest theory of selection, relying on purely linear arguments, is investigated for the amplitude equation (where a transition to absolute instability is predicted) and for the starting equations. The comparison gives the expected result that the predictions of the amplitude equation are good only near the threshold. The early breakdown of the equation is primarily related to the fact that the small modulation expansion of the linear-stability spectrum is actually an expansion in powers of $\beta\kappa$. As a result we find that the transition to absolute instability does not take place near the param-

eters predicted by the amplitude equation. However, it is possible that such a transition may take place through other scenarios for which the linear analysis cannot account. We describe one such possibility that arises owing to the multiplicity of the linear front branches and argue that the nonlinear front solution corresponding to the crossing point of the two branches may be the selected front. In this case, the transition to absolute instability does take place near the threshold. It is also important to mention that, in the experiments, the spatial content of the pump beams plays an important role: When the pump beams are simple plane waves, conical light scattering appears to develop instead of phase-conjugate beams.[15] Only when enough spatial information is added to the pump beam is the phase-conjugate beam propagating in the backward direction with respect to the incident wave obtained. So experimentally the physical problem is two dimensional only when the pump beams have enough spatial information, i.e., the pump beams diffract before exiting the crystal. We are therefore cautious in referring to the simple four-wave-mixing geometry studied above as a double-phase-conjugate mirror. However, the gain mechanism for the conical rings is the same grating-sharing process, and the formation of the conical rings is attributed to the multiplicity of the perfectly shared gratings in the third dimension. At present the effects of diffraction on the underlying physics is unclear. The amplitude-equation formalism, allowing the treatment of both modulation and nonlinearity, provides a possible scheme to investigate this phenomenon theoretically.

In conclusion, we have derived an amplitude equation that governs the spatio-temporal behavior of the 2D-grating amplitude in the nonlinear regime, near the threshold. The equation renders the very difficult study of the nonlinear dynamical problem much more manageable. The regime in which the equation is expected to work well is described.

APPENDIX A: DERIVATION OF THE AMPLITUDE EQUATION

Here we extend the linear analysis in Section 3 to the nonlinear regime. The formulation presented below[22] is a standard perturbative approach to systems that exhibit spatial instability near a critical point. The approach has been rediscovered in many different contexts and bears a strong resemblance to the mean-field Landau theory of equilibrium phase transitions. Near the threshold the nonlinearities are weak, and the spatial and temporal modulations of the most unstable mode become slow. The balance between these effects is described by the amplitude equation. In what follows we will derive this equation for the regime $\beta \gg 1$ (thick hologram). This derivation follows in close analogy with that in the appendix in Ref. 3.

We first express the right- and left-moving-wave amplitudes in Eqs. (1b) and (1c) as a sum of the pump and scattered waves:

$$A = \overline{A_p}(z, t)\exp(-jx) + a(z, x, t), \qquad \text{(A1a)}$$

$$B = \overline{B_p}(z, t)\exp(-jx) + b(z, x, t). \qquad \text{(A1b)}$$

In our notation the bar on the amplitudes implies that the amplitude depends only on z and, the amplitudes $\overline{A_p}$, $\overline{B_p}$ keep track of the depletion of the pump beams. In this notation the intensity profile is given by $i = 1 + 1/2(\overline{A_p^*}a + \overline{B_p^*}b)$ + c.c.

Near the transition point we define a perturbation parameter $\varepsilon = (\gamma_0 - \gamma_{0c})/\gamma_{0c}$, and we wish to separate fast and slow scales for x and t. The slow scales of the modulation are defined as

$$X = \varepsilon^{1/2}x, \quad T = \varepsilon t. \qquad \text{(A2)}$$

We will consider a, b, e… to be given by products of the functions of fast and slow variables. From the chain rule for differentiation we therefore must make the replacements

$$\partial_x \rightarrow \partial_x + \varepsilon^{1/2}\partial_X, \quad \partial_x \rightarrow \partial_t + \varepsilon\partial_T. \qquad \text{(A3)}$$

In this analysis (to the order we take the expansion) ∂_X terms will show up only in linear terms in the amplitude equation, which will come about at $O(\varepsilon^{3/2})$. These linear coefficients can be inferred from the linear-stability analysis. For convenience we will ignore these terms in the present derivation and refer back to the linear-stability analysis for their contributions. We now expand Eqs. (1) consistently in $\varepsilon^{1/2}$:

$$a = \varepsilon^{1/2}a_0 + \varepsilon a_1 + \dots \qquad \text{(A4a)}$$

$$b = \varepsilon^{1/2}b_0 + \varepsilon b_1 + \dots \qquad \text{(A4b)}$$

$$e = \varepsilon^{1/2}e_0 + \varepsilon e_1 + \dots \qquad \text{(A4c)}$$

$$i = 1 + \varepsilon^{1/2}i_0 + \varepsilon i_1 + \dots \qquad \text{(A4d)}$$

$$\overline{A_p} = 1 + \varepsilon\overline{A_{p1}} + \dots \qquad \text{(A4e)}$$

$$\overline{B_p} = 1 + \varepsilon\overline{B_{p1}} + \dots \qquad \text{(A4f)}$$

At $O(\varepsilon^{1/2})$ Eqs. (1a) and (1b) are of the form

$$L\begin{pmatrix} e_0 \\ a_0 \\ b_0 \end{pmatrix} + \begin{pmatrix} \alpha\partial_x i_0 \\ j2\gamma_{0c}e_0\exp(-jx) \\ -j2\gamma_{0c}e_0\exp(-jx) \end{pmatrix} = 0, \qquad \text{(A5)}$$

where the linear operator L is defined as

$$L = \begin{pmatrix} 1 - \alpha^2\partial_x^2 & 0 & 0 \\ 0 & \partial_z - j\beta - j\beta\partial_x^2 & 0 \\ 0 & 0 & \partial_z + j\beta + j\beta\partial_x^2 \end{pmatrix}, \qquad \text{(A6)}$$

and the solution at this order is the phase-conjugate mode:

$$a_0 = \overline{a_0}\exp(jx) = j(1 + 4\alpha^2)/\alpha A_0(T)z\exp(jx), \quad \text{(A7a)}$$

$$b_0 = \overline{b_0}\exp(jx) = j(1 + 4\alpha^2)/\alpha A_0(T)(1 - z)\exp(jx), \qquad \text{(A7b)}$$

$$e_0 = \overline{e_0} \exp(2jx) + \text{c.c.} = A_0(T)\exp(2jx) + \text{c.c.},$$
(A7c)

where we allow the amplitude of the threshold solution A_0 to vary with the slow time scale T. Here, $\overline{a_0}$, $\overline{b_0}$, $\overline{e_0}$ are solutions to the linear equation (identical to the linearized 1D theory):

$$L_0\begin{pmatrix}\overline{e_0}\\\overline{a_0}\\\overline{b_0}\end{pmatrix} = \begin{pmatrix}1 & j\widetilde{\gamma}/2 & j\widetilde{\gamma}/2\\j2\gamma_{0c} & \partial_z & 0\\-2\gamma_{0c} & 0 & \partial_z\end{pmatrix}\begin{pmatrix}\overline{e_0}\\\overline{a_0}\\\overline{b_0}\end{pmatrix}.$$
(A8)

The boundary conditions are $\overline{a_0}(0) = 0$, $\overline{b_0}(1) = 0$. At the first nonlinear order, $O(\varepsilon)$, the depletion of the pump beams appear:

$$\partial_z\begin{pmatrix}1 & 0\\0 & 1\end{pmatrix}\begin{pmatrix}\overline{A_{p1}}\\\overline{B_{p1}}\end{pmatrix} = j2\gamma_{0c}\begin{pmatrix}\overline{a_0}\,\overline{e_0^*}\\-\overline{b_0}\,\overline{e_0^*}\end{pmatrix},$$
(A9a)

$$\begin{pmatrix}\overline{A_{p1}}\\\overline{B_{p1}}\end{pmatrix} = -|A_0(T)|^2(1 + 4\alpha^2)^2/\alpha^2\begin{pmatrix}z^2\\(1-z)^2\end{pmatrix}.$$
(A9b)

At this order we also have

$$L\begin{pmatrix}e_1\\a_1\\b_1\end{pmatrix} + \begin{pmatrix}\alpha\partial_x i_1\\j2\gamma_{0c}e_1\exp(-jx)\\-j2\gamma_{0c}e_1\exp(-jx)\end{pmatrix}$$

$$= \begin{pmatrix}-\alpha e_0\partial_x e_0 - e_0 i_0 - \alpha^2\partial_x e_0\partial_x i_0 + \alpha^2 i_0\partial_x^2 e_0\\-j2\gamma_{0c}e_0 a_0\\j2\gamma_{0c}e_0 a_0\end{pmatrix}.$$
(A10)

Notice that on the right there are no secular terms of the

corrections from these terms to be of order Γ/β^2 and emphasize the point that these terms have to be considered for very small angles between the two pump beams (the thin hologram limit). However, the nonlinear terms in the first row with x dependence of the form $\exp(4jx)$ are not necessarily small, and we have to keep the contributions from these terms. With the above considerations the solutions at this order can be expressed as

$$a_1 = \overline{a_1}\exp(jx), \qquad b_1 = \overline{b_1}\exp(jx),$$

$$e_1 = \overline{e_{10}}\exp(2jx) + \overline{e_{11}}\exp(4jx) + \text{c.c.}$$
(A11)

The homogeneous problem for $\overline{e_{10}}$, $\overline{a_1}$, $\overline{b_1}$ is identical to the problem at $O(\varepsilon^{1/2})$, and $\overline{e_{11}}$ can be calculated from Eq. (A10) in a straightforward manner:

$$\overline{e_{11}} = -jA_0(T)^2/(2\alpha)(1 + 8\alpha^2)/(1 + 16\alpha^2).$$
(A12)

Notice that this grating, at double the most unstable wave number, comes from the nonlinear terms in the material equation (1a) and not from higher diffraction orders.

At $O(\varepsilon^{3/2})$ we introduce seed noise to the problem at the boundaries: $\overline{a_2}(0) = s_2$, $\overline{b_2}(1) = s_2$. We define $\overline{a_{2s}}$, $\overline{b_{2s}}$ as $\overline{a_2} = \overline{a_{2s}} + s_2$, $\overline{b_2} = \overline{b_{2s}} + s_2$ so that the linear problem for $\overline{a_{2s}}$, $\overline{b_{2s}}$ will have the same boundary conditions as in Eq. (A8). This introduces an additional term in the intensity distribution:

$$i_2 = i_{20} + i_{21} + i_s = 1/2(\overline{a_{2s}} + \overline{b_{2s}})\exp(2jx)$$

$$+ 1/2(\overline{A_{p1}^*a_0} + \overline{B_{p1}^*b_0}) + s_2\exp(2jx) + \text{c.c.}$$
(A13)

With the above definitions Eqs. (1) become

$$L\begin{pmatrix}e_2\\a_{2s}\\b_{2s}\end{pmatrix} + \begin{pmatrix}\alpha\partial_x i_{20}\\j2\gamma_{0c}\overline{e_{20}}\exp(-jx)\\-j2\gamma_{0c}\overline{e_{20}}\exp(-jx)\end{pmatrix} = \begin{pmatrix}\{-\partial_t\overline{e_0} - \overline{e_{11}}\,\overline{i_0^*}(1 + 24\alpha^2) - 2j\alpha(\overline{e_{11}}\,\overline{e_0^*} + \overline{e_0^2 i_0^*} + \overline{i_{21}} + s_2)\}\exp(2jx) + \text{c.c.}\\(-j2\gamma_{0c}\overline{e_0 A_{p1}} - j2\gamma_{0c}\overline{e_0})\exp(jx)\\(j2\gamma_{0c}\overline{e_0 B_{p1}} + j2\gamma_{0c}\overline{e_0})\exp(jx)\end{pmatrix}.$$
(A14)

form $[\exp(2jx), \exp(jx), \exp(jx)]$. In the second and third rows of this equation the nonlinear terms that depend on the fast variable x, varying as $\exp(3jx)$ or $\exp(-jx)$, correspond to higher diffraction orders. For $\beta \gg 1$ it can be

Here on the right only the secular terms are shown. With similar considerations the amplitudes e_2, a_2, b_2 can be expressed as in Eq. (A11) with amplitudes $\overline{e_{20}}$, $\overline{e_{21}}$. The secular part of Eq. (A14) becomes

$$(1 + 4\alpha^2)L_0\begin{pmatrix}\overline{e_{20}}\\\overline{a_{2s}}\\\overline{b_{2s}}\end{pmatrix}$$

$$= \begin{pmatrix}-\partial_T A_0 + A_0|A_0|^2(1 + 28\alpha^2 + 208\alpha^4 + 512\alpha^6)/[(1 + 16\alpha^2)4\alpha^2] - A_0|A_0|^2(1 + 4\alpha^2)^3[z^3 + (1-z)^3]/(\alpha^2) - 2j\alpha s_2\\-jA_0|A_0|^2(1 + 4\alpha^2)^4/\alpha^3 z^2 + jA_0(1 + 4\alpha^2)/\alpha\\+jA_0|A_0|^2(1 + 4\alpha^2)^4/\alpha^3(1 - z^2) - jA_0(1 + 4\alpha^2)/\alpha\end{pmatrix}.$$
(A15)

shown that these terms are strongly phase mismatched to the most unstable mode and can be neglected. We expect

We would like to invert this equation but since the operator on the left has vanishing eigenvalues we must impose

a solvability condition, which requires that the vector on the right should not drive any eigenvector of the operator with zero eigenvalue. The condition for this is that the vector on the right-hand side, which we must now find, be orthogonal to the eigenvector with zero eigenvalue of the adjoint operator. The eigenvalue equation for the adjoint system (for zero eigenvalue) is of the form

$$
L_0^+ \begin{pmatrix} \overline{e_0^+} \\ \overline{a_0^+} \\ \overline{b_0^+} \end{pmatrix} = \begin{pmatrix} 1 & -j2\gamma_{0c} & j2\gamma_{0c} \\ -j\widetilde{\gamma}/2 & -\partial_z & 0 \\ -j\widetilde{\gamma}/2 & 0 & -\partial_z \end{pmatrix} \begin{pmatrix} \overline{e_0^+} \\ \overline{a_0^+} \\ \overline{b_0^+} \end{pmatrix} = 0,
$$
(A16)

with boundary conditions $\overline{b_0^+}(0) = 0$, $\overline{a_0^+}(1) = 0$. The eigenvector is given by

$$
\begin{pmatrix} \overline{e_0^+} \\ \overline{a_0^+} \\ \overline{b_0^+} \end{pmatrix} = \begin{pmatrix} 1 \\ -j\{\alpha/(1+4\alpha^2)\}(z-1) \\ -j\{\alpha/(1+4\alpha^2)\}z \end{pmatrix}.
$$
(A17)

The inner product for the linear system is defined as

$$
\langle (x_1, x_2, x_3) | (y_1, y_2, y_3) \rangle = \int_0^1 \mathrm{d}z \sum_i^3 x_i^* y_i.
$$
(A18)

The solvability condition requires the left-hand side of Eq. (A15) to be orthogonal to the adjoint eigenvector, Eq. (A17). The orthogonality condition results in the following amplitude equation:

$$
-\partial_T A_0 + A_0(1 + 4\alpha^2) - j2\alpha s_2 + A_0|A_0|^2
$$
$$
\times \left\{ \frac{(1 + 28\alpha^2 + 208\alpha^4 + 512\alpha^6)}{[(1 + 16\alpha^2)4\alpha^2]} - \frac{(1 + 4\alpha^2)^3}{(3\alpha^2)} \right\}.
$$
(A19)

Returning to the unscaled units and expressing the amplitude as the amplitude for one of the scattered waves rather than the grating [Eqs. (A7)] we arrive at the general amplitude equation $\{A = \varepsilon^{-1/2} A_0[-j\alpha/(1 + \alpha^2)], \partial_T = \varepsilon^{-1}\partial_t, s = \varepsilon^{-3/2} s_2\}$:

$$
\tau_0 \partial_t A = \varepsilon A + 2s - g_0 |A|^2 A.
$$
(A20)

APPENDIX B: DERIVATION OF EQ. (1A)

In this section we present a sketch of the derivation of Eq. (1a) from the basic equations for the photorefractive effect with a single charge carrier; see Ref. 9, Subsection 3.2.1. Equation (1a) has also been studied in Ref. 7. In general it can be shown that for fast electronic recombination ($\mathrm{d}n/\mathrm{d}t = 0$, n is the electron-number density), the basic equations can be reduced to a single equation for the space-charge field. Here, we consider the case for which only a small fraction of the donor-number density is ionized ($N_D \gg N_A$) and neglect dark conduction. We also consider the open circuit case where the total current density is zero. Under these conditions the basic equations can be reduced to the following set of equations:

$$
\partial_t e + ne + \partial_x n = 0,
$$
(B1)

$$
\partial_x e = N^+ - 1,
$$
(B2)

$$
nN^+ = i.
$$
(B3)

Here, the acceptor-number density N^+ and n are normalized by N_A, which is the number density of negative ions that compensate for the charge N^+ in the dark, and the zeroth-order solution for the electron-number density [n_0, Ref. 9, Subsection 3.2.1, Eq. (3.10)], respectively. The first equation, Eq. (B1), is derived from the continuity equation and Poisson's equation for the open-circuit case. The equation states that the total current density (the sum of the displacement-, drift-, and diffusion-current densities from left to right) is zero. Equation (B2) is Poisson's equation for fast electronic recombination [$|n_0 n| \ll |N_A(N^+ - 1)|$]. The last equation, Eq. (B3), is derived from the rate equation for the acceptor-number density for $N_D \gg N_A$.

The acceptor-number density can be eliminated from these equations by a simple substitution. The transformed Eq. (B2) can be solved for the electron-number density, which in turn can be substituted into Eq. (B1). Carrying out the spatial derivative for the electron-number density and multiplying the equation by $(1 + \partial_x e)^2$ results in Eq. (1a). Equation (1a) can be thought of as a continuity equation. The time-derivative term in Eq. (1a) arises from the displacement-current density. The first term on the left and the second term on the right arise from the drift-current density, and the remaining terms arise from the diffusion-current density.

*M. C. Cross is also with Condensed Matter Physics, California Institute of Technology, 114-36, Pasadena, California 91125.

REFERENCES

1. S. Weiss, S. Sternklar, and B. Fischer, Opt. Lett. **12**, 114 (1987).
2. D. Engin, S. Orlov, M. Segev, A. Yariv, and G. Valley, Phys. Rev. Lett. **74**, 1743 (1995); M. Goulkov, S. Odoulov, and R. Trott, Ukr. Phys. J. **36**, 7, 1007 (1991).
3. M. C. Cross and P. C. Hohenberg, Rev. Mod. Phys. **65**, 851 (1993).
4. A. A. Zozulya, Opt. Lett. **16**, 545 (1991); V. V. Eliseev, V. T. Tikhoncuk, and A. A. Zozulya, J. Opt. Soc. Am. B **8**, 12 (1991).
5. O. V. Lyubomudrov and V. V. Shkunov, Kvant. Elektron. (Moscow) **19**, 1102 (1992); S. Sternklar, Opt. Lett. **20**, 3 249 (1995).
6. D. Shaw, Opt. Commun. **94**, 458 (1992).
7. A. A. Zozulya, M. Saffman, and D. Z. Anderson, Phys. Rev. Lett. **73**, 6,818 (1994).
8. M. Cronin-Golomb, Opt. Commun. **89**, 276 (1992); M. Segev, D. Engin, A. Yariv, and G. C. Valley, Opt. Lett. **18**, 1828 (1993); A. A. Zozulya, M. Saffman, and D. Z. Anderson, J. Opt. Soc. Am. B **12**, 255 (1995); M. R. Belic, J. Le-

onardy, D. Timotijevic, and F. Kaiser, J. Opt. Soc. Am. B **12**, 9 (1995).

9.   P. Gunter and J.-P. Huignard, eds., *Photorefractive Materials and Their Applications* (Springer-Verlag, Berlin, 1989), Vol. 1, Chaps. 2 and 3.

10. N. Kukhtarev, Sov. Tech. Phys. Lett. **2**, 438 (1976).

11. H. Kogelnik, Bell Syst. Tech. J. **48**, 2909 (1969).

12. N. A. Korneev and S. L. Sochava, Opt. Commun. **115**, 539 (1995).

13. M. Segev, D. Engin, A. Yariv, and G. C. Valley, Opt. Lett. **18**, 956 (1993).

14. N. V. Bobodaev, V. V. Eliseev, L. I. Ivleva, A. S. Korshunov, S. S. Orlov, N. V. M. Polozkow, and A. A. Zozulya, J. Opt. Soc. Am. B **9**, 1493 (1992).

15. A. P. Mazur, A. D. Novikov, S. G. Odulov, M. S. Soskin, and M. V. Vasnetov, J. Opt. Soc. Am. B **10**, 1408 (1993); Q. B.

He, P. Yeh, C. Gu, and R. R. Neurgaonkar, J. Opt. Soc. Am. B **9**, 114 (1992).

16. M. Saffman, D. Montgomer, A. A. Zozulya, K. Kuroda, and D. Z. Anderson, Phys. Rev. A **48,** 4, 3209 (1993).

17. W. van Saarloos and P. C. Hohenberg, Physica D **56**, 303 (1992).

18. M. C. Cross, Phys. Rev. Lett. **57**, 2935 (1986).

19. W. van Saarloos, Phys. Rev. A **39**, 6367 (1989).

20. A. Kolmogorov, I. Petrovsky, and N. Piskunov, Bull. Univ. Moscow, Ser. Int. Sec. A **1**, 1 (1937); D. G. Aronson and H. F. Weinberger, *Partial Differential Equations and Related Topics*, J. A. Goldstein, ed. (Springer-Verlag, Heidelberg, 1975), p. 5.

21. E. M. Lifshitz and L. P. Ptiaevskii, *Physical Kinetics* (Pergamon, New York, 1981), Vol. 10, Chap. 6.

22. A. C. Newell, Lect. Appl. Math. **15**, 157 (1974).